

Review

Not peer-reviewed version

Hydrogen Combustion:Features and Barriers to its Exploitation in the Energy Transition

[Eugenio Giacomazzi](#)^{*} , Guido Troiani , Antonio Di Nardo , Giorgio Calchetti , [Donato Cecere](#) , [Giuseppe Messina](#) , Simone Carpenella

Posted Date: 27 September 2023

doi: 10.20944/preprints202309.1834.v1

Keywords: hydrogen combustion; hydrogen blends; power generation; gas turbines; hard-to-abate industry



Preprints.org is a free multidiscipline platform providing preprint service that is dedicated to making early versions of research outputs permanently available and citable. Preprints posted at Preprints.org appear in Web of Science, Crossref, Google Scholar, Scilit, Europe PMC.

Copyright: This is an open access article distributed under the Creative Commons Attribution License which permits unrestricted use, distribution, and reproduction in any medium, provided the original work is properly cited.

Disclaimer/Publisher's Note: The statements, opinions, and data contained in all publications are solely those of the individual author(s) and contributor(s) and not of MDPI and/or the editor(s). MDPI and/or the editor(s) disclaim responsibility for any injury to people or property resulting from any ideas, methods, instructions, or products referred to in the content.

Review

Hydrogen Combustion: Features and Barriers to Its Exploitation in the Energy Transition

Eugenio Giacomazzi ^{*,†,‡}, Guido Troiani [‡], Antonio Di Nardo [‡], Giorgio Calchetti [‡], Donato Cecere [‡], Giuseppe Messina [‡] and Simone Carpenella [‡]

Laboratory of Processes & Systems Engineering for Energy Decarbonisation, ENEA, 00123 Rome, Italy

* Correspondence: eugenio.giacomazzi@enea.it

† Current address: Casaccia Research Center, TERIN-PSU-IPSE, S.P. 081, ENEA, Via Anguillarese 301, S.M. Galeria, 00123 Rome, Italy.

‡ These authors contributed equally to this work.

Abstract: The aim of this article is to review hydrogen combustion applications within the energy transition framework. Hydrogen blends are also included, from the well known hydrogen enriched natural gas (HENG) to the hydrogen and ammonia blends whose chemical kinetics is still not clearly defined. Hydrogen and hydrogen blends combustion characteristics will be firstly summarized, in terms of standard properties like the laminar flame speed and the adiabatic flame temperature, but also evidencing the critical role of hydrogen preferential diffusion in burning rate enhancement and the drastic reduction in radiative emission with respect to natural gas flames. Then, combustion applications in both thermo-electric power generation (based on internal combustion engines, i.e., gas turbines and piston engines) and hard-to-abate industry (requiring high temperature kilns and furnaces) sectors will be considered, highlighting the main issues due to hydrogen addition related to safety, pollutant emissions, and potentially negative effects on industrial products (e.g., glass, cement and ceramic).

Keywords: hydrogen combustion; hydrogen blends; power generation; gas turbines; hard-to-abate industry

1. Introduction

According to the International Energy Agency, energy efficiency, behavioural change, electrification, renewables, hydrogen and hydrogen-based fuels, and CCUS are the key pillars to decarbonise the global energy system [1]. The increasing share in cumulative emission reductions due to hydrogen justifies its important role in the Net zero Emissions Scenario [1] to decarbonise sectors where emissions are hard-to-abate, such as heavy industry and long distance transport. Within the power sector, hydrogen holds the potential to deliver flexibility by aiding in the management of increasing proportions of fluctuating renewable energy generation. Additionally, it can play a role in enabling seasonal energy storage, further enhancing the versatility and reliability of the energy system.

Hydrogen stands out as an exceptionally versatile fuel that can be generated using a wide spectrum of energy sources, encompassing coal, oil, natural gas, biomass, renewables, and nuclear power. The production methods are equally diverse, spanning processes like reforming, gasification, electrolysis, pyrolysis, water splitting, and numerous others. In recent times, distinct colors have been assigned to signify different pathways of hydrogen production: "green" for hydrogen extracted through electrolysis with electricity from renewable sources; "grey" for H₂ produced from fossil raw materials such as natural gas (this generates around 10 tons of CO₂ per ton of H₂); "blue" for production derived from fossil fuels with carbon capture, utilization, and storage (CCUS); "turquoise" for H₂ produced by splitting natural gas at high temperatures (only solid carbon is produced in the process, i.e., no CO₂ is emitted if the process runs on heat from renewable energy sources). Due to the multitude of energy sources that can be employed, the environmental consequences associated with each method

of hydrogen production can differ significantly. Moreover, the geographic location and the specific configuration of the process also play a crucial role in shaping these environmental impacts.

As of 2020, the worldwide demand for hydrogen amounted to approximately 90 million metric tons (Mt) [1], indicating a growth of 50% since the year 2000. Nearly the entirety of this demand is attributed to applications in refining and industrial sectors. Refineries, on an annual basis, utilize nearly 40 million metric tons of hydrogen for tasks such as feedstock and reagents, as well as an energy source.

Demand is slightly elevated in the industrial sector, surpassing 50 million metric tons (Mt) of hydrogen [1]. This demand is primarily attributed to its use as feedstock. Within the chemical production sector, approximately 45 million metric tons of hydrogen are consumed, with roughly three-quarters allocated to ammonia production and the remaining one-quarter directed towards methanol production. The remaining 5 million metric tons of hydrogen find usage in the direct reduced iron (DRI) process for steelmaking. This allocation of demand has remained nearly unchanged since 2000, with only a marginal uptick in demand noted for DRI production.

Simultaneously, mounting concerns about climate change have led to heightened awareness, prompting both governments and industries to make resolute pledges aimed at curtailing emissions. While this has expedited the integration of hydrogen into novel applications, the demand in this realm still remains quite limited. For instance, in the transport sector, the yearly hydrogen demand stands at less than 20 thousand metric tons (kt) of hydrogen, representing a mere 0.02% of the overall hydrogen demand. As illustrated in the IEA roadmap for achieving a net-zero state by 2050 [2], the attainment of government decarbonization objectives will necessitate a significant and abrupt acceleration in the adoption of hydrogen technologies across various segments within the energy sector.

In the Net Zero Emissions Scenario [2], the demand for hydrogen experiences a substantial increase, expanding nearly six times its current value to reach 530 million metric tons (Mt) of hydrogen by the year 2050. This surge in demand is divided, with half of it being allocated to the industry and transport sectors. In this scenario, the presence of hydrogen in the power sector undergoes a marked increase. Its utilization in gas-fired power plants and stationary fuel cells plays a crucial role in mitigating the challenges associated with the growing output from variable renewable sources, facilitating the integration of larger proportions of solar photovoltaic (PV) and wind energy, and furnishing seasonal energy storage solutions. Additionally, hydrogen's application in buildings also encounters growth, although its adoption remains constrained to specific circumstances. In the same scenario projected for 2050, approximately one-third of the hydrogen demand is allocated to the production of hydrogen-based fuels. These fuels include ammonia, synthetic kerosene, and synthetic methane. Current applications of ammonia are primarily centered around nitrogen fertilizers, but now the interest is growing in other sectors, such as long-distance shipping of hydrogen and combustion, where co-firing of ammonia in coal-fired power plants has shown successful demonstrations; however, further research, development, and deployment efforts are necessary to advance the utilization of pure ammonia as a direct fuel source (also thermally and catalytically decomposed) in steam or gas turbines.

When hydrogen is burned, the primary resultant is water (H_2O), rendering it a genuinely emission-free fuel in terms of CO_2 . The ultimate objective is to utilize 100% green hydrogen for combustion, supplanting natural gas entirely. In the interim, a more immediate goal involves blending hydrogen with natural gas to be used in gas turbines and other industrial combustion applications, thereby achieving a partial reduction in CO_2 emissions. Nowadays, the term fuel-flexibility refers to combustion-based power generation systems (especially gas turbines) capability to operate with hydrogen blends as fuel in a stable, safe and reliable way when the H_2 content unpredictably varies in time due to intermittent production from renewables. Such blends range from hydrogen-enriched natural gas (HENG) to ammonia (a promising H_2 -carrier).

An important aspect, easy to understand but very often neglected is that large hydrogen mass fractions are required in fuel mixtures to significantly affect CO_2 emissions. Talking in terms of volume

fractions is a common practice, but in a methane/hydrogen mixture the H₂ volume percentage largely differs from its mass counterpart, as shown in Figure 1; for example, 30 and 50% vol. correspond just to 5 and 11% mass, while 80% vol. is required to reduce CO₂ emissions by 55%. However, even the low 30% vol. becomes really challenging if significant temporal fluctuations of composition are considered.

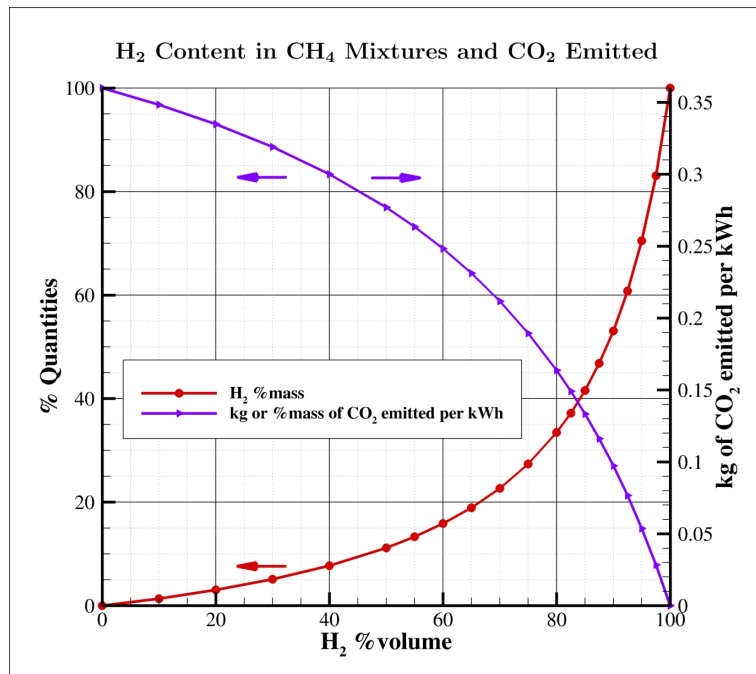


Figure 1. Relation between volume and mass percentages in methane/hydrogen mixtures, and impact in terms of CO₂ emitted (assuming an electrical efficiency of 55%). The percentage quantities on the left are with respect to pure methane.

Adopting hydrogen in combustion application is not straightforward. A fuel consisting in 100% hydrogen necessitates an extra volumetric flow of 208%, approximately three times more than that needed for methane to have the same power; hence, depending on the blend percentage, there might be a need to expand the size of piping and valves to manage the higher volumetric flow demanded by hydrogen. Its physical characteristics introduce complexities in terms of production, storage, and transportation, setting it apart from natural gas. Safety issues also arise due to hydrogen's broader flammability range, lower vapor density, and faster flame speed, necessitating careful consideration within the framework of system design. Safety mechanisms for gas detection and fire protection must be adjusted to address hydrogen's unique volatility and distinctive detection characteristics. Correspondingly, measures for explosion-proofing should be equipped to confine more substantial explosions, and modifications to ventilation systems are essential. Moreover, hydrogen encounters distinctive challenges related to supply and infrastructure. The fuel system's pipelines and valves enclosed must harmonize with hydrogen, necessitating materials that are hydrogen-compatible and designed with safety factors in mind. Additionally, the design must incorporate hydrogen-tight seals capable of accommodating the small hydrogen gas molecules.

In this article, combustion features of hydrogen enrichment in fuel blends will be firstly considered, also briefly looking at effects on materials. Then, an overview of combustion applications in power generation and hard-to-abate sectors will be provided to identify the state-of-the-art and the barriers for its exploitation. In the end, conclusions and future directions will be drawn.

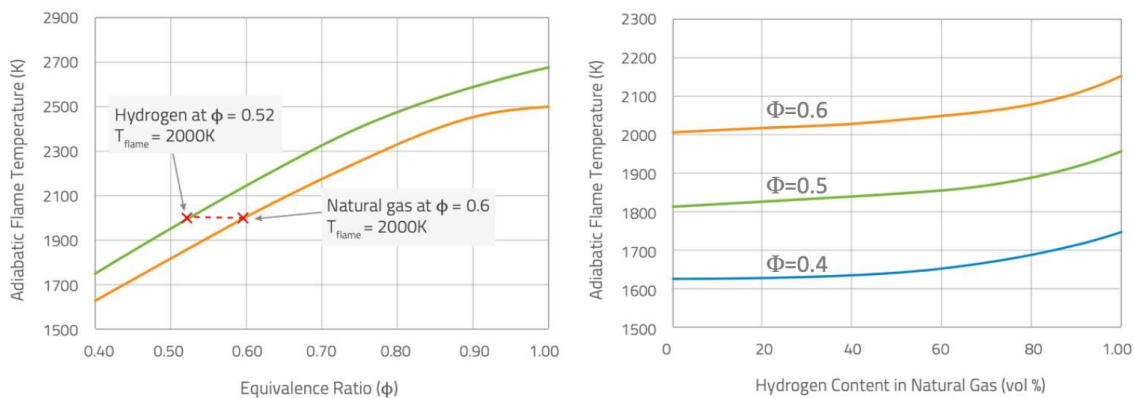


Figure 2. Adiabatic flame temperature *vs* equivalence ratio (Φ) for hydrogen and methane flames in air (left), and *vs* hydrogen content for some specific mixtures (right) [3].

2. Features of Hydrogen Combustion

When employing hydrogen either alongside natural gas or as a complete substitute, it's crucial to grasp the distinctions between these two fuels.

Hydrogen possesses a density that is one-ninth that of natural gas, and it holds the distinction of being the smallest known molecule. This characteristic introduces challenges regarding transportation and sealing. Furthermore, hydrogen's heating value is merely one-third that of natural gas (on volumetric basis), signifying that three times the amount of hydrogen fuel is necessary to generate an equivalent power output compared to natural gas. In the combustion of hydrogen, while more volume flow is required for the same energy production, approximately 20% less air by volume is required to produce a flame comparable to natural gas, thus reducing the mass flow through the combustor and consequently the convective heat transfer. Under this perspective, flue gas recirculation can be used to increase the mass flow of air into the combustor, increasing convective heat transfer and reducing the flame temperature [4–6].

Moreover, hydrogen has a considerably broader flammability range than natural gas, leading to heightened concerns regarding environmental, health, and safety aspects during both hydrogen transportation and combustion. Hydrogen largely enhances the reactivity of fuel blends: the ignition delay time decreases [7,8]; at room temperature and pressure the flammability limits (0.1–7.1) are well wider than those of natural gas (0.5–1.67); the flame speed is higher [9] and the critical strain rate increases, thus reducing potential flame quenching [10,11]. At fixed equivalence ratio (Φ), the hydrogen/air premixed flame burns with an adiabatic flame temperature higher than the corresponding natural gas one (see Figure 2, left). In the same way, fixing the equivalence ratio, the increase of the hydrogen content in a methane/hydrogen mixture can rise the adiabatic flame temperature (see Figure 2, right).

The higher hydrogen combustion temperatures produce an increase of nitrogen oxides, NO_x , most of which is thermal, i.e., coming from high temperature regions with sufficiently long residence time [12]. This is one of the main concerns in operating burners with fuel blends having high H_2 content.

2.1. Effects on Flame Stability

Combustion in excess of air can mitigate NO_x production [13], but at these conditions of extremely lean combustion, the gaseous mixtures rich in hydrogen are characterized by a disparity between the diffusion by mass and the thermal one, inducing phenomena of intrinsic instability with a strong impact on the laminar and turbulent combustion speed, thus altering the flame topology.

These effects have been predicted theoretically [14–16], and also visualized experimentally [17,18] and numerically (numerical simulations) [19–21]. In particular, these reactive mixtures are extremely sensitive to some external perturbations (usually present in every burner) producing exponential

growths in the extension of the flame front, in pressure fluctuations, as well as in temperature, with a negative impact on the performance of thermal machines, their polluting emissions and even their life time. However, with an accurate design of the combustion chamber, it is possible to maximize the advantages deriving from these instabilities, i.e., the increase in the average combustion speed (and therefore in the thermal power) and compactness of flames (smaller size of the devices), while eliminating or mitigating the negative aspects, such as high pressure and temperature fluctuations, localized quenching and flashbacks.

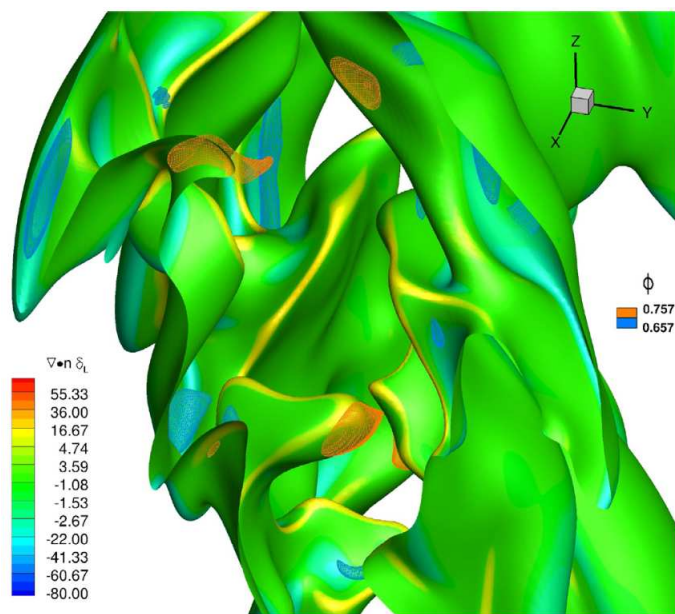


Figure 3. Snapshot of a progress variable iso-surface associated to the maximum heat release coloured with its normalized curvature and two iso-surfaces of equivalence ratio at $\Phi = 0.657$ (blue) and $\Phi = 0.757$ (orange), respectively, for a CH_4/H_2 – air flame at a nominal $\Phi = 0.7$ and $X_{\text{H}_2} = 0.2$ [22].

Hydrogen, and light species in general, diffuse preferentially with respect to other species in a mixture. In recent decades, so-called asymptotic theories have been developed which predict the existence of perturbations (in specific wavelength ranges) particularly effective in destabilizing combustion processes, which strongly depend on the Lewis number of the mixture. The Lewis number (Le) represents a measure of the disparity between thermal and mass diffusivity, through their ratio: therefore a hydrogen-rich mixture, which has a mass diffusivity extremely greater than the methane molecule, will be characterized by a Lewis number less than unity. In premixed combustion, this makes local equivalence ratio lower or higher than the inlet nominal equivalence ratio of the considered fuel blend depending on the local flame curvature. An example is provided in Figure 3 for a CH_4/H_2 – air flame at a nominal $\Phi = 0.7$ and 20% H_2 volume content [22], where the instantaneous flame surface (identified by means of the progress variable value related to the maximum heat release) is shown evidencing local hydrogen enrichment in positive curvature regions, and a decrease of equivalence ratio in negative curvature regions. This mechanism changes flame speed locally, and tends to enhance the wrinkling of the flame front and the burning rate.

Mixtures with Lewis numbers smaller than a critical value (Le_c , generally less than one) will be characterized by small-scale (thermo-diffusive) and large-scale (hydro-dynamic) instabilities. With a Lewis number close to the Le_c or greater, mainly hydro-dynamic instabilities will survive. This type of instability is based on different formation mechanisms. In the case of thermo-diffusive instabilities, the high diffusivity of the mixture (in particular of H_2) will give rise, when the flame front is perturbed/corrugated, to inhomogeneity of the equivalence ratio of the mixture and of the local temperatures with a consequent variation of the local laminar combustion speeds, which in turn will amplify the initial perturbations of the front, making it even more corrugated. Such corrugations

increase the turbulent flame speed, as shown in Figure 4 that reports the ratio between the turbulent and laminar flame speeds of a premixed CH₄/H₂/Air Bunsen flame: the lower the Lewis number and the higher the turbulence intensity, the higher the turbulent flame speed will be [23].

This phenomenon is more effective the more the perturbations, and the corrugations of the front are of small scale. In the case of $Le > Le_c$ this phenomenon is strongly limited, and what arises is a hydro-dynamic type mechanism, in which the large-scale corrugations of the front compress or expand the stream lines of the flow field, thus channeling areas with low or high velocity upstream of the flame front. Also this mechanism tends to amplify initially small amplitude perturbations.

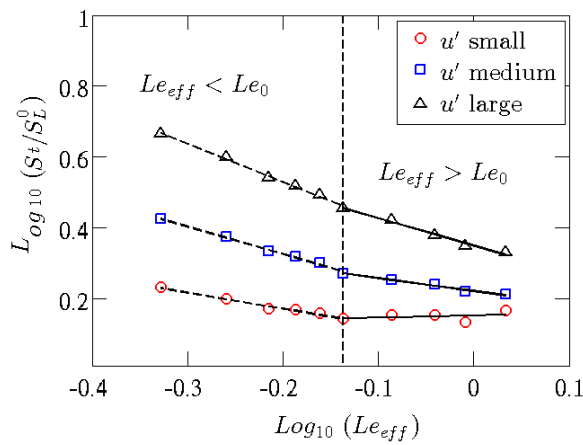


Figure 4. Ratio between turbulent and laminar flame speed versus the effective Lewis number [23] in a premixed CH₄/H₂/Air Bunsen flame, parameterized with turbulence intensity of the jet [24].

The presence of thermo-diffusive instabilities alone is not possible. In fact, being the hydro-dynamic instability a phenomenon always present in a flame, due to the difference in temperature between reactants and combustion products, that of the thermo-diffusive type is driven by the disparity between mass and thermal diffusivity, which can be eliminated by acting on the composition of the reactant mixture. Studies present in literature have shown the interaction, in Bunsen geometries, of hydrodynamic instabilities with flow turbulence [25–29], while the characterization of the interaction of turbulence with both instabilities (hydro-dynamic and thermo-diffusive) still lacks.

Given its higher combustion temperature and faster flame speed, hydrogen combustion can lead to instability and an increased risk of flameouts and flashback events. In particular, the high reactivity of hydrogen inherently increases the risk of self-ignition and flashbacks in the premix section. The problem becomes even more important in systems with very high inlet air temperatures [30,31], as in highly recuperated gas turbines. Furthermore, compared to natural gas flames, hydrogen flames exhibit significantly different thermoacoustic behavior due to higher flame velocity, shorter ignition delay, and distinct flame stabilization mechanisms, resulting in different flame shapes, different positions and different reactivity. Therefore, the risk of combustion dynamics (self-sustained oscillations at the acoustic frequency of the combustion chamber) in gas turbines running on hydrogen enriched fuels is higher than in natural gas operation [32,33]. This implies that undesirable and dangerous phenomena such as combustion instability, flashbacks and lean-blowouts, can occur not only at steady state, but also during transient regimes, for example when the power changes rapidly and/or the fuel composition varies.

2.2. Effects on Pollutant Emissions

The main emission indicators on which the performance of burners are based are mainly nitrogen oxides NO_x, composed of NO and NO₂, CO and carbon dioxide CO₂.

There is no fundamental chemical kinetic reason why H_2 flames should produce more NO_x than natural gas flames. Since most of NO_x is thermal, i.e., produced where reactants are at high temperature for a sufficiently long residence time (above a certain threshold temperature, around 1800 K, the production of NO_x increases dramatically), more lean mixtures have to be adopted to reduce peak temperatures (see Figure 2) when burning fuel blends with higher H_2 content.

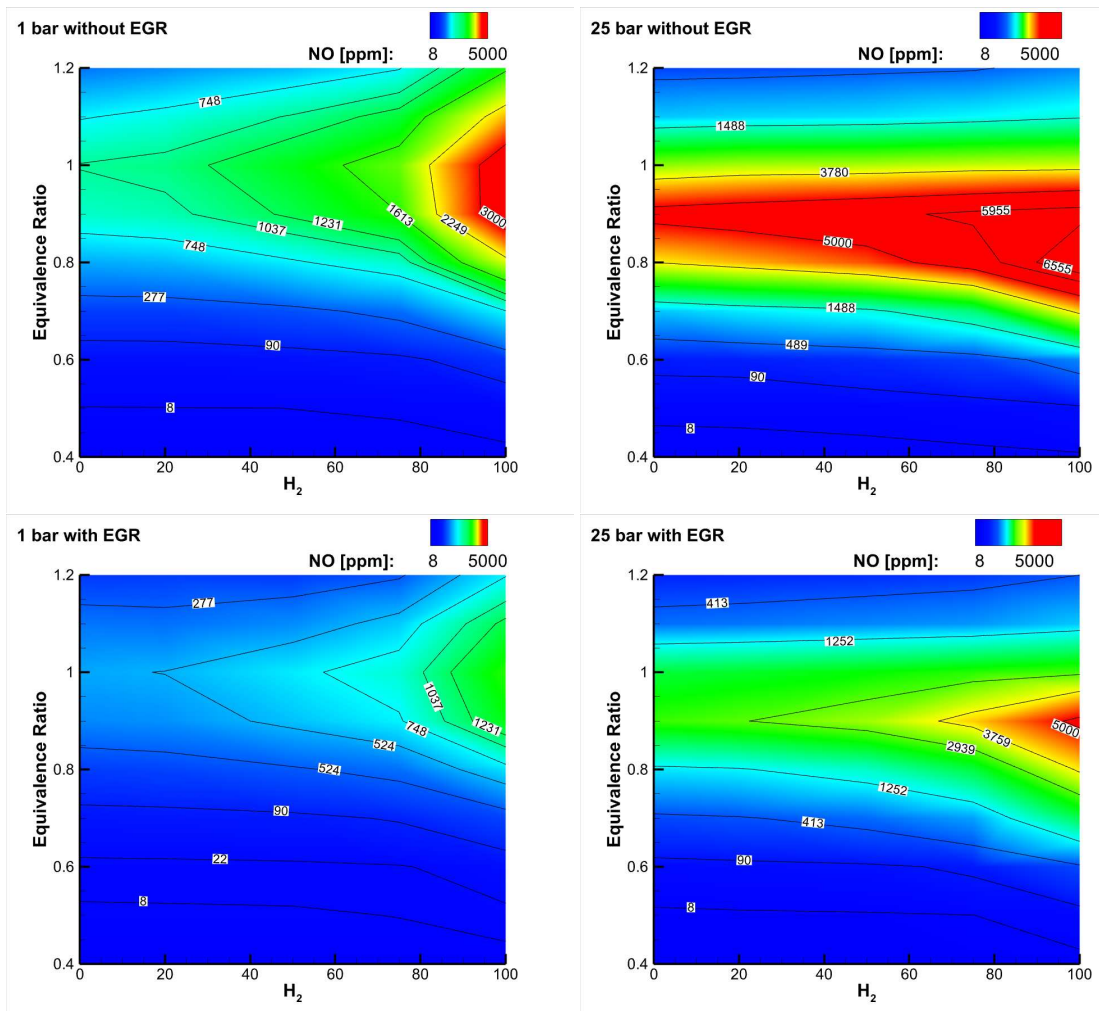


Figure 5. NO_x emissions in ppm vs equivalence ratio and hydrogen content for a CH_4/H_2 blend reacting with air without and with dilution through exhaust gas recirculation (EGR). Two pressures are considered: 1 bar (left) and 25 bar (right). The initial temperature of reactants changes with the hydrogen content: without EGR it is in the range 750 – 820 K, and with EGR it is in the range 800 – 850 K, decreasing while H_2 is increased [34].

Figure 5 (top) shows a map of NO_x emissions as a function of the equivalence ratio and hydrogen content for a CH_4/H_2 blend reacting with air at two different pressures [34]: respecting NO_x emission limits requires to operate at an equivalence ratio well below 0.5, especially at high H_2 content and high pressure. Implementation of exhaust gas recirculation (EGR) can be of help in reducing NO_x emissions in different applications (see Figure 5, bottom), and in gas turbines it is a potential solution to enhance their turn-down ratio, i.e., to reduce their partial load (minimum technical environmental load).

Apart from NO_x predictions and expectations from chemical kinetics calculations, some direct measurements of NO_x emissions in a specific premixed Bunsen burner at 1 atmosphere are here reported due to the interesting operational strategy implemented to avoid flashback occurrence [35]: as the hydrogen content increases in the CH_4/H_2 fuel blend, driving to the increase of flame propagation speed, the value of the equivalence ratio is decreased by increasing the excess air. This strategy

allowed to maintain the flame propagation speed constant (0.33 m/s) and at the same time lowered the adiabatic flame temperature; besides, the power was kept constant (7.1 kW) by raising the flow rate of the reactant mixture. Such a strategy avoided flashback up to the maximum jet Reynolds number (explored range, 10.000-13.900) in [35]: it would be interesting to see what happens at higher turbulent jet Reynolds numbers to check the effects on the non-linear increase of the turbulent flame speed. The measurements of emissions were carried out at the chimney, taking a small quantity of combustion products and analyzing them by means of the FTIR (Fourier transform infrared spectroscopy) technique. [36,37].

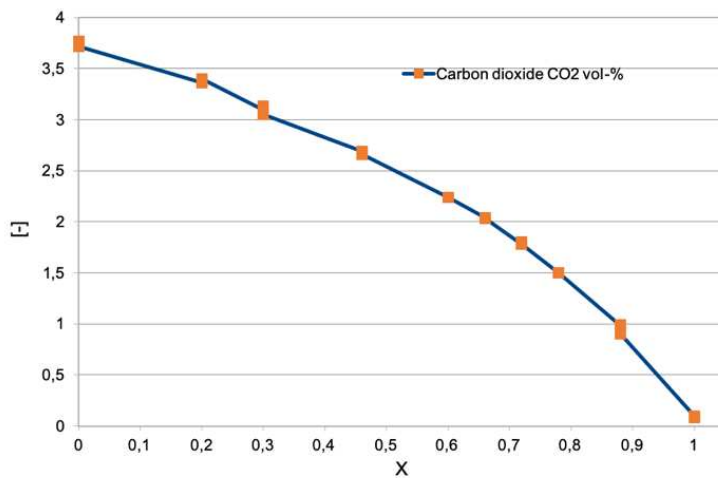


Figure 6. CO₂ concentration at varying hydrogen content.

Figure 6 shows the results of the sampling of the carbon dioxide emitted [35]. As the percentage of hydrogen, expressed as molar fraction, increases (0, pure methane; 1, pure hydrogen), the carbon dioxide content drops until it reaches zero when the mixture is made up of only hydrogen and air. Results are in agreement with the chemiluminescence emission described later in Figures 10 and 11. As expected from data in Figure 1, the presence of carbon dioxide is significant even at very high H₂ mole fraction values.

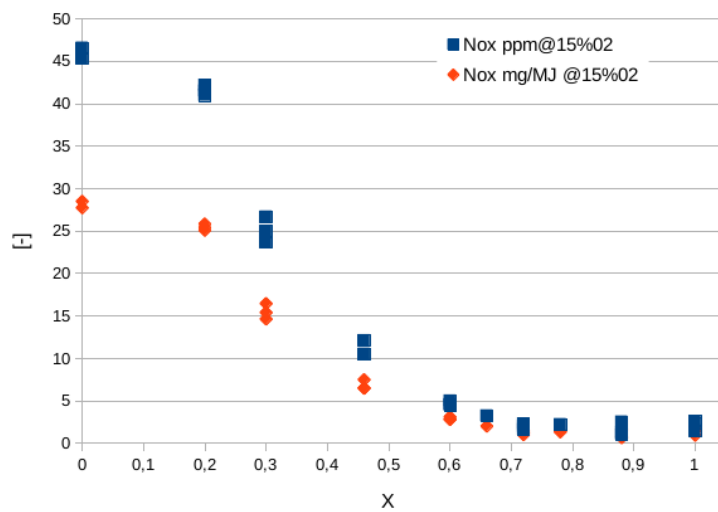


Figure 7. NO_x concentration (ppm) and (mg/MJ) as the hydrogen content varies. Values are scaled at an oxygen content of 15% [35].

Figure 7 shows the quantity of NO_x expressed in parts per million (ppm), scaled to a value of oxygen in the combustion equal to 15%, and also in mass normalized by the the fuel energy actually converted into heat, to take into account the different composition of exhausts while increasing the hydrogen content [35]. Besides, in this way the emission values of machines of significantly different sizes (power) can be compared. It is observed that above a hydrogen mole fraction of 45-50%, emissions decrease dramatically. This is due to the regulation strategy adopted in [35]: while hydrogen content is increased, the equivalence ratio is decreased thus lowering the flame temperature and thermal NO_x contribution (the most relevant). In fact, temperature changes from about 2100 K for the methane flame to nearly 1600 K for the hydrogen one.

2.3. Effects on Radiant Energy Transfer

The Radiative Transfer of Energy (RTE) is a very important mechanism in several applications: high-pressure and high-temperature engine combustion chambers, rocket propulsion, hypersonic vehicles, spacecraft atmospheric reentry, ablating thermal protection systems, glass manufacturing, plasma generators, nuclear fusion.

Notably, hydrogen flames are significantly less visible than those produced by natural gas, due to the reduced concentration of radiant species such as soot, CO_2 and radicals. This makes flame detection a more intricate endeavour; infrared flame detection is ineffective for a hydrogen flame, which means an ultraviolet system is required [38–41]. At the same time, this affects also the radiative heat transfer from the flame, with important implications in some applications, such as glass furnaces. The lower emissivity and lower mass flow rate (less air is required while increasing H_2 content) of the combustor therefore change the heat transfer balance.

Radiative absorption properties depend on the absorption coefficient κ_λ that in gases often varies strongly with wavelength, temperature and pressure. It also increases proportionally to the concentration of the participating species. While solid surfaces can be assumed opaque, gas absorption or emission properties are very irregular in the wavelength domain, being significant only in certain wavelength regions, especially at temperature below a few thousand Kelvin. When the temperature increases, the absorption coefficient of cold lines decreases but hot lines appear at high wavelengths, slightly increasing the absorption coefficient. Increasing pressure causes spectral line broadening, that is mainly due to molecular collisions [42] and can produce wider and more overlapping lines than at lower pressures: as a consequence, the gas becomes "grayer" (opaque) and the spectral absorption coefficient amplitude largely increases, as shown in Figure 8 [43, p. 138] or reported in [44]. An appropriate and convenient mean absorption coefficient to account for the total emission from a volume element of absorbing medium is the Planck mean absorption coefficient, that depends only on the local properties and can be tabulated. Today, the Planck mean absorption coefficient estimated in the past [42, p. 253-324], can be more accurately calculated [45] directly from high-resolution spectroscopic databases, such as HITRAN [46] and HITEMP [47]: the new databases produce absorption coefficients generally larger than those obtained through older databases, especially at higher temperatures and pressures.

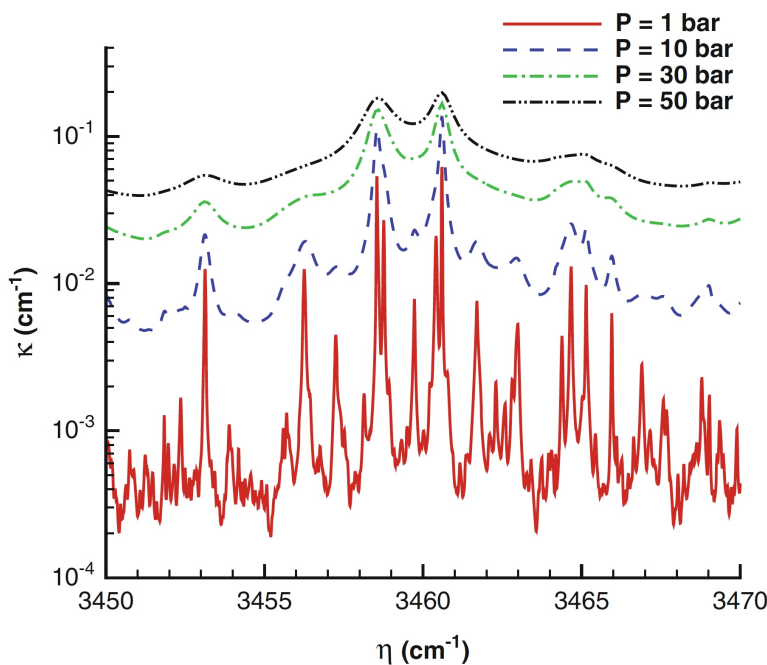


Figure 8. Wide band absorption coefficient spectra of a mixture containing 1% CO₂ and 2% H₂O [43, p. 138].

At industrial furnace and combustion chamber temperatures the gaseous species that absorb and emit significantly are CO₂, H₂O, CO, SO₂, NO, and CH₄. Other gases, such as N₂, O₂ and H₂, are transparent to infrared radiation and do not emit significantly; however, they become important absorbing/emitting contributors at very high temperatures. A non-negligible contribution to radiation is also provided by hot carbon (soot) particles within the flame and from suspended particulate material (as in pulverized-coal combustion).

Concerning flames, it is well known that neglecting radiation at atmospheric pressure conditions may lead to overprediction of temperature of up to 200 K. However, it has to be noted that numerical predictions strongly depend on the RTE model adopted: the usually-employed optically-thin or gray radiation models lead to underprediction of temperature of up to 100 K and more [48,49]. Furthermore, radiation is enhanced by turbulence through strong nonlinear interactions between temperature and radiative property fluctuations (TRI): such interactions increase the heat loss from a flame leading to a reduction in the local gas temperature of 200 K and more. The TRI cooling effect is even enhanced in high-pressure combustors that typically exhibit larger optical thicknesses [50,51].

For systems where RTE is important, radiation was shown to be equivalent to a large nonlinear diffusion term: in fact, the radiant transfer of heat can work as a preheating mechanism as conduction of heat, thus resulting in higher flame speeds [52]. As an example, Figure 9 shows an instantaneous distribution of the radiative source term in the energy equation in a non-premixed cyclonic combustor [53] burning air and hydrogen in MILD combustion regime. The source term is estimated by means of the M1-radiation model [54]: its distribution reveals regions exhibiting heat losses (negative radiative source term) or preheating effects (positive source). The distribution of the radiative source term versus temperature is also shown at the bottom of the same figure, coloured by means of the OH radical mass fraction: higher temperature reacting regions with higher OH concentrations loose heat, while colder non-reacting regions (jets, identifiable in the planar section of Figure 9, top) with lower OH content are preheated.

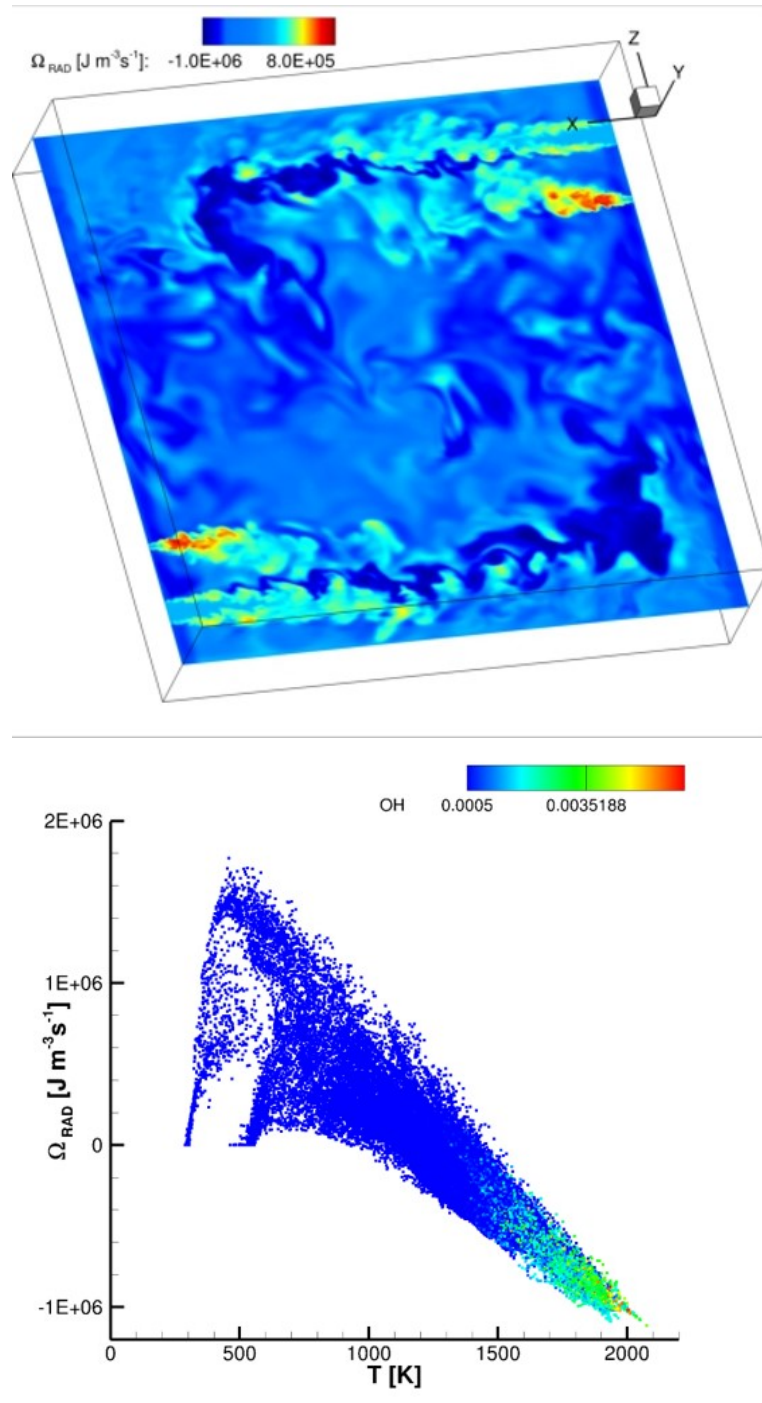


Figure 9. Instantaneous spatial distribution on a planar section of a cyclonic combustor burning hydrogen and air in non-premixed MILD combustion regime [53]. The distribution shown at the bottom is coloured by means of the OH radical mass fraction.

Focusing on peak flame temperature, radiation typically reduces it in low pressure flames. Although radiation effects become more pronounced as the pressure is increased (due to increased emission/absorption), the peak flame temperature is less affected by radiation because of the faster chemical reactions, as also observed in [43, p. 139]. In fact, according to the Arrhenius law, the chemical reaction rate is proportional to reactant molar concentrations raised to a power that is equal to the number of moles that have to collide for the reaction to occur. Hence, the reaction rate is proportional

to p for first-order reactions and to p^2 for second-order reactions; three-body reactions, are even more enhanced [55].

It is known that hydrogen flames have lower emissivity than natural gas flames. Such radiative emission changes may have important implications in some applications [56].

In [35] a series of premixed Bunsen flames at constant 7.1 kW thermal power, burning methane and hydrogen in air at atmospheric pressure with increasing hydrogen content, were experimentally investigated. While increasing the hydrogen content, the thermal power was kept constant maintaining the same laminar flame speed of the fuel mixture (hence, decreasing its equivalence ratio) and increasing the flow rate (hence, the jet Reynolds number). The spectrum of the electromagnetic radiation emitted was measured in a range of wavelengths between 200 and 1080 nm (nanometer), from ultraviolet to near infrared. The radiation emitted was collected by a system of lenses capable of focusing the image of the flame in an area of about 1-2 cm, where it was collected by an integrating sphere and sent, through an optical fibre, to a digital spectrometer. The integrating sphere is a spherical device which has the ability to concentrate almost all of the radiation collected inside it through a hole of about 1 cm made on its surface: measurement details can be found in [35,57]. The result is that, by integrating the measurement over a rather large surface of flame, the spatial dependence of the measurement is substantially lost, highlighting the spectral dependence on the wavelengths and the type of mixture.

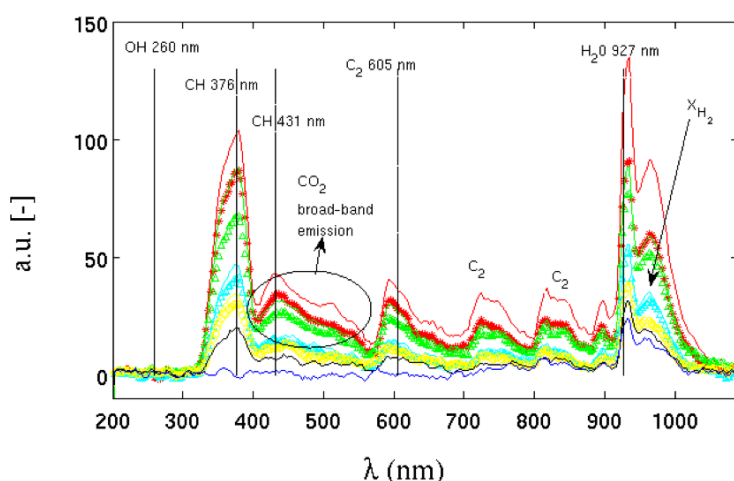


Figure 10. Emission spectrum at different hydrogen contents. The X_{H_2} arrow points to the increasing direction of the hydrogen molar fraction.

Figure 10 shows the spectra of radiant energy emitted by flames in [35] with increasing hydrogen contents. The arrow with X_{H_2} defines the direction in which the molar fraction of hydrogen in the methane/air mixture increases. It starts from a pure methane flame, up to a pure hydrogen flame. The figure also shows the spectral emission lines of the major emitting species. As the carbon content in the mixture decreases, the decrease in energy emitted by the species CH, CO₂, C₂, H₂O and H₂ is evident.

As the hydrogen content in the mixture increases, the contribution of carbon to the emission of radiative energy progressively decreases until, in the mixture of pure hydrogen, only the emission peak of water and H₂ survives, strongly reducing the ratio between radiant/convective energy emitted. In all the mixtures, the emission peak of the OH radical, located in the ultraviolet around a wavelength between about 260 and 310 nm, is substantially absent, despite being a chemical species strongly present inside the flame front. According to the authors in [35], the reason for this absence could lie in the low sensitivity of the instrument at those wavelengths such as to return a signal-to-noise ratio that is too low for this type of measurement. Even with this lack, the differences in radiant energy emitted with the presence or absence of methane are considerable.

A lower radiative emission translates into a greater quantity of energy which is transmitted by convection, which mainly follows an axial direction, whereas the radiative one is emitted in all directions, and, given the cylindrical symmetry of the flame, preferentially in a radial direction. While this is beneficial for gas turbine applications (lower heat losses to walls and less cooling issues), it could be a serious issue in other industrial applications like raw-material melting kilns or product cooking kilns.

In the same experiments [35], the temperature of a strongly absorbing metal body (black coloured) positioned on the flame side at a distance of about 2 diameters D (D, the diameter of the Bunsen burner adopted) was measured by a thermocouple. The correlation between the radiant energy emitted in radial direction and temperature is shown in Figure 11. It can be seen that as the hydrogen content increases, the value of the integral of the radiative emission (I) is linearly anti-correlated with the temperature reached by the absorbent body. It can be deduced that the reduction of the chemical species that emit by chemiluminescence strongly influences the amount of radiative thermal energy emitted. It is also observed that up to a hydrogen volume content of 78% (30% by mass of hydrogen) this phenomenon is strongly limited: even a minimal quantity (in volume) of methane is sufficient to "colour" the flame, which emits over a more extensive range of wavelengths; the flame is instead almost colourless when the carbon is absent.

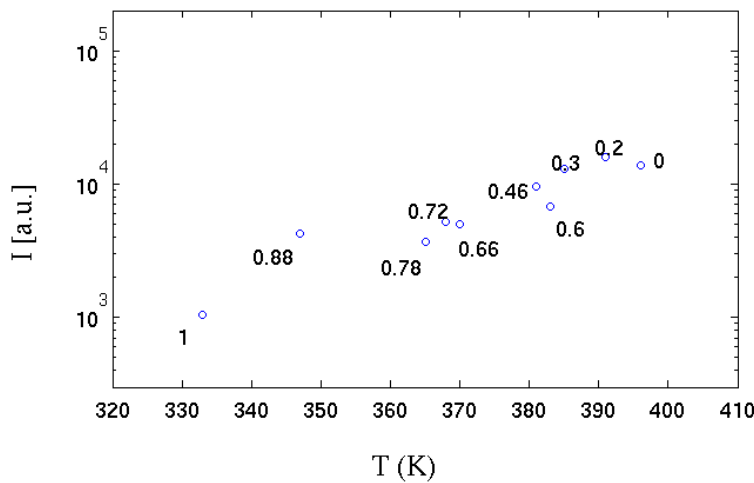


Figure 11. Integrated emission spectrum (over all wavelengths) for the various hydrogen contents vs temperature measured in the radial direction [35]. Each experimental point is labelled with molar fraction of hydrogen. See Figure 1 for the equivalence between hydrogen mass and volume fraction.

2.4. Effects on Materials

Besides affecting combustion characteristics, hydrogen enrichment to natural gas also affects materials. Hydrogen is absorbed by some containment materials and piping, which can cause loss of ductility or embrittlement. Hydrogen embrittlement becomes evident shortly after its introduction into a system and is an irreversible process. This phenomenon diminishes the material's yield stress, consequently compromising its fatigue resilience, particularly under low-cycle fatigue conditions [58]. The extent and rapidity of embrittlement is accelerated by factors such as high temperature, pressure, and stress levels. It's important to note that not all materials exhibit the same susceptibility to hydrogen embrittlement. Stainless steels and nickel alloys, which are frequently employed in gas turbine combustion systems, are particularly prone to heightened embrittlement at elevated temperatures. This complicates the selection of materials for combustion hardware, weld joints, and braze joints due to the need to mitigate the effects of hydrogen embrittlement.

A 100% hydrogen flame is shorter and located much closer to the burner than a methane flame under the same operating conditions, due to the higher flame speed and shorter ignition times [22]. Conversely, industrial experience suggests that with high percentages of water or steam added to the fuel, the flame length can increase significantly. Also this factor, combined with the increase in flame temperature, has important implications on the potential impact on combustor materials [59]. The most significant worry concerning hot gas path components arises from the fact that hydrogen's elevated combustion temperature leads to a rise in turbine firing temperature. Furthermore, the gas temperature profile upon leaving the combustor will be hotter and exhibit distinct characteristics when burning hydrogen in comparison to natural gas. This heightened firing temperature and alterations in the combustion profile shape will necessitate modifications in the designs of component cooling and coatings to avert any reduction in part lifespan.

It is also important to consider that the combustion of hydrogen changes the composition of the exhaust gases compared to the use of natural gas. The change in the composition of the combustion products can have a significant impact in direct combustion equipment, where the combustion gases come into direct contact with the objects that are being produced [60,61]. In direct fired equipment where the flue gases are mixed with large amounts of fresh air before coming into contact with the product (e.g. dryers operating at 200°C), this is unlikely to be a major problem, although further tests are timely. However, in some applications such as glass kilns or lime kilns, the flue gases are not mixed before contact with the product; therefore, changes in the flue gas composition could affect the quality of the product itself [61], for example by influencing the volatility of sulphate in glass furnaces. Of particular concern is the increased moisture content of flue gases [61] and the possible effects this could have within furnaces and other direct fired equipment [56].

3. Gas Turbine and Piston Engines Power Generation

Although natural gas currently stands as the most environmentally friendly option among major combustion fuels, employing it contributes to roughly 20% of the total CO₂ emissions, with nearly 15% for power generation in the United States [62]. Hydrogen is a viable fuel option for both reciprocating gas engines and gas turbines to reduce CO₂ emissions, but its use in power generation is negligible at present, accounting for less than 0.2% of the electricity supply [1].

Although the most advanced gas reciprocating (or piston) internal combustion engines are capable of accommodating gases containing hydrogen content of up to 70% on a volumetric basis [63] and several manufacturers have showcased the feasibility of engines that operate using 100% hydrogen (anticipated to become commercially accessible in the near future), they can be generally fed with a fraction of about 30%, going beyond 50% by adjusting compression and power in some cases. The main problems are the increased explosion limits and tendency to detonate, and the increased size of the fuel injection system, which can lead to a downgrading of engine displacement by more than 30%. Other issues include increased NO_x emissions. This may require the installation of catalytic exhaust systems, which are already used in some gas engines.

Thermo-electric power generation with gas turbines is one of the most immediately applicable solutions for reducing CO₂ emissions. Although this, a significant share of CO₂ emissions in the power generation sector can be attributed to gas turbines: utilizing hydrogen combined with natural gas will progressively become more significant in the effort to decrease CO₂ emissions. While renewable energy sources are making progress on the global energy stage, gas turbines will maintain their prominence in power generation both during the energy transition period and in the future energy scenario with an increasing percentage of non-programmable renewable sources, thanks to their capability to provide flexibility to the electric grid system [64,65]. In this vision, it has to be accepted that, over the years, the very concept of the gas turbine will undergo a natural evolution, adapting to the technological advances offered by the market. Flexibility of gas turbines gathers both their "load-flexibility" or "operational flexibility", and their "fuel-flexibility" [66]. The load-flexibility refers to gas turbine capability to change its power in small time to quickly stabilize the electric grid. Different solutions

were proposed and implemented in the recent years [67–69], reaching today a power rate of 10% of nominal power per minute. Such a value seems to be fine for gas turbine users today and should be maintained in the future moving to hydrogen gas turbines. The fuel-flexibility refers instead to gas turbine capability to operate with different fuels, and more specifically for the present time, with fuel blends with varying hydrogen content [70]. However, despite the considerable efforts and investments made by the various manufacturers in recent years, the actual fuel-flexibility of the machines, i.e. their stable, efficient, clean, reliable and safe operation from 100% natural gas to 100% hydrogen with varying hydrogen content, is a challenge yet to be overcome due to technological issues in the combustion system.

Hydrogen strongly alters combustion characteristics of a reacting mixture with respect to natural gas: the ignition delay time decreases, the flammability limits enlarge, the laminar flame speed increases, the turbulent flame speed becomes faster and pressure dependent [71,72], the adiabatic flame temperature increases. Hence, apart from issues related to its production, storage (lower vapor density), and transportation, safety issues also arise from such changes. In particular, the broader flammability range amplifies the potential for fuel ignition within the mixing passages; combustion dynamics can be dramatically affected by dangerous flashbacks due to the increased flame speed [73] and/or thermos-acoustic instabilities [74,75] that may drive to unplanned overhauls thus reducing system reliability. Although both research and industrial sectors have been investigating the combustion instability topic for many years, it is still a not fully solved problem: strategies commonly adopted to avoid or limit the dangerous effects of such instabilities in modern gas turbines are based on empirical methods. Besides, the effects of hydrogen content on combustion dynamics make the Wobbe index unreliable for its applicability as fuel interchangeability index [76]. During transient operations, such as start-up and shutdown, these dynamics become a primary concern. Implementation of advanced sensors for real-time combustion monitoring can be a key requirement [77,78]. For the foreseeable future, the inclusion of a safe fuel like natural gas will remain necessary for non-steady operations such as startup, shutdown, and part-load scenarios. Start-up procedures are commonly based on natural gas or liquid fuels, combining diffusive and premixed combustion at least up to FSNL (Full Speed No Load) state. At present, an average of 5% H₂ by volume is tolerated at start-up. In essence, the stable operability window for many lean premixed combustors becomes narrower due to these dynamics.

Special attention has to be given to control temperature peaks to limit NO_x emission; maintaining them below the current natural gas limits of 25 ppmv appears challenging for gas turbines operating in the range 0-100% H₂ up to 2030: this is a difficult task due to the easily reached higher temperatures. It is observed that hydrogen changes exhaust gas composition (more water) and also the gas turbine power should be considered. For these reasons, there is an open discussion in gas turbine associations and OEMs about how to take into account such operating conditions in the law limits: a very promising suggestion to discuss with regulatory entities is to quantify such emissions as the ratio between the mass of NO_x at the exit and the input fuel energy [mg/MJ] [79].

Another important effect of burning fuel mixtures with high H₂ content is the higher steam content in the exhausts. This increases the heat exchange in the hot path of the gas turbine, thus requiring more cooling [80] and reducing component life cycle due to increased risk of hot corrosion. As a consequence, reducing the turbine inlet temperature, and consequently reducing the machine power with penalty losses of 2% points in efficiency (another challenging limit to maintain up to 2030), is a commonly adopted solution [81].

Furthermore, using a blend with 100% hydrogen necessitates an extra volumetric flow of 208%, approximately three times more than that needed for methane, making the direct and seamless utilization of hydrogen in gas turbines challenging.

In the end, necessary modifications in design are highly contingent on the proportion of hydrogen intended for combustion. The utilization of hydrogen can be categorized into groups based on the volume percentage: low (5-10%), medium (10-50%), and high (more than 50%) blends. Turbines operating with a low hydrogen blend may not necessitate design alterations, as the fuel-burning

characteristics closely resemble those of a pure natural gas stream. In the case of medium blends, the overall architecture and combustor of the turbine might remain largely unchanged, but adjustments to combustor materials, fuel nozzles, and control systems will be essential. The development of retrofit solutions for existing gas turbines is certainly a key factor. When dealing with higher hydrogen blends, exceeding 50%, extensive modifications to the turbines become imperative, and a comprehensive retrofit of the combustion system is likely required. Numerous original equipment manufacturers (OEMs) are presently engaged in developing new combustion systems capable of accommodating elevated hydrogen blend levels.

Hence, as the proportion of hydrogen in the fuel increases, an unmodified combustion system encounters greater challenges. Compounding these difficulties, in the foreseeable future, combustion systems will need to retain both fuel flexibility and the capability to burn natural gas.

While research is very advanced for low levels of hydrogen, it is significantly less so for high levels. The state of the art on hydrogen combustion is based on two combustion modes: diffusion flames with nitrogen, water or steam as diluent and lean premixed flames.

In combustion systems with a diffusion flame and addition of diluents, it is possible to handle up to 100% vol. of hydrogen. However, these systems have several disadvantages, including reduced efficiency compared to systems without dilution, higher NO_x levels compared to lean premix technology, greater plant complexity and thus higher construction and maintenance costs.

Table 1. State of the art for gas turbines on the volume percentage accepted by the combustor [82]

Combustion	H ₂ % vol.	NO _x Complexity CAPEX/OPEX
Non-premixed / Diluted	0-100%	higher
DLE lean premixed comb.	~44-63% heavy duty (100-500 MWe) ~ 43 – 55% industrial (30-100 MWe) ~35% aero-derivative (1-30 MWe) ~20-32% microturbine (0.1-1 MWe)	

Dry premixed combustion technology (Dry Low-Emission, DLE) does not implement any dilution; it has greater potential, but is not yet mature enough for very high hydrogen contents or when greater flexibility of the fuel mix is required (e.g., to use natural gas/hydrogen mixtures with an H₂ content of 0 to 100%). The maximum permissible hydrogen concentration varies widely between manufacturers. Table 1 shows the levels of hydrogen currently accepted by the different classes of gas turbines [82,83], from heavy-duty, to industrial, to aero-derivative and microturbines (20% vol. H₂ refers to the lowest powers). The reason lies in the different combustion temperatures and technologies used in the different classes. With reference to micro-gas turbines, despite the efforts of some OEMs, they do not follow the learning curve of the heavy-duty ones at the same pace, having a very tiny hydrogen tolerance. However, being the micro-gas turbines users of the same gas grid of larger ones, more efforts on R&D are mandatory to reach the same hydrogen compliance.

Currently, there are no fuel-flexible DLE machines on the market capable of handling the entire 0-100% range of hydrogen mixed with natural gas. The technical experience accumulated with high hydrogen syngas (30 and 60% vol. of H₂ and CO), revisited and adapted, has proved useful. As a result, most gas turbine manufacturers offer units originally developed for syngas applications, which can also be used for natural gas/hydrogen mixtures with high H₂ levels (around 60% vol.). Looking at OEMs' catalogues, the stat-of-the-art exhibits, on average, DLE (Dry Low Emission) gas turbines able to burn H₂ up to 30% by volume with low NO_x emissions (<25 ppmv at 15% O₂). Due to the higher flame temperatures with respect to natural gas, in some cases NO_x emissions are controlled only by derating the machine, i.e., reducing its power [83]; besides, it must be said that the strongest NO_x limitations for natural gas (<15 ppmv at 15% O₂) are not always reached today: as an example, Ansaldo Energia GT36 and GT26 gas turbines could tolerate respectively up to 50% and 30% of hydrogen by volume with a 15 ppmv compliance, but AE94.3A and AE94.2 could tolerate up to 25% of hydrogen by volume

with a 25 ppmv compliance. Hence, most of investments are on DLE technology, i.e., lean premixed combustion without dilution (steam, nitrogen, water), also for retrofit solutions. New combustion concepts are also explored, such as the sequential combustion at constant pressure (implemented in the GT36) [67,84] and that based on micro-mixing [85] and exhaust gases recirculation (EGR) [5,6].

Table 2. Key Performance Indicators for DLE gas turbines [82]. NO_x refers to NO + NO₂. The maximum electrical efficiency loss refers to the Full-Speed Full-Load condition in Combined Cycle Gas Turbines. The minimum ramp rate is referred to the Full-Load condition.

KPI	Unit	SoA 2020	Target 2024	Target 2030
H ₂ fuel content	% by mass % by volume	0-5 0-30	0-23 0-70	0-100 0-100
NO _x emissions	ppmv at 15%O ₂ dry mmg/MJ _{fuel}	<25 at 30% vol. H ₂ <31 at 30% vol. H ₂	<25 at 70% vol. H ₂ <29 at 70% vol. H ₂	<25 at 100% vol. H ₂ <24 at 100% vol. H ₂
Max. H ₂ content at start-up	% by mass % by volume	0.7 5	3 20	100 100
Max. electrical efficiency loss	% points	10 at 30% vol. H ₂	10 at 70% vol. H ₂	10 at 100% vol. H ₂
Min. ramp rate	% load / minute	10 at 30% vol. H ₂	10 at 70% vol. H ₂	10 at 100% vol. H ₂
H ₂ accepted fluctuations	% by mass / minute % by volume / minute	±1.4 ±10	±2.21 ±15	±5.11 ±30

Table 2 shows the KPIs (Key Performance Indicators) for DLE gas turbines with reference to the state of the art (SoA) in 2020 and with forecasts to 2024 and 2030. It is noted that maintaining the same NO_x limits from 30 to 100% H₂ is already a challenge; moreover, the commonly adopted normalisation for NO_x to 15% O₂ under dry conditions (without H₂O) cannot be applied to fuels with very different reactivity and combustion products than natural gas; a more appropriate normalisation is that suggested in the same table, which uses the mass of NO_x in mg per quantity of fuel energy injected in MJ; this new normalisation was suggested not only in the SRIA2021-2027 of the Clean Hydrogen Partnership [82], but also in the Hydrogen Working Group of the European Turbine Network [3]. As far as start-up is concerned, it should be noted that this phase is typically carried out with only natural gas or liquid oil.

4. Hard-to-Abate Industry

Comprising 38% of the total final energy demand, the industrial sector stands as the most substantial end-use segment. Notably, this sector is responsible for 26% of the global energy system's CO₂ emissions [1]. Involving processes heavily relying on fossil fuels, the hard-to-abate sector is the most challenging in reducing pollutant emissions [56,86]: electrification is not a straightforward solution in most of the related industrial processes and the potential implementation of hydrogen opens some critical issues on the process itself and on the quality of the product. Within the industrial landscape, hydrogen plays a role in utilizing 6% of the overall energy demand. This hydrogen is predominantly employed as feedstock in chemical production and as a reducing agent in the manufacturing of iron and steel. The annual industrial demand for hydrogen amounts to 51 million metric tons [1].

Table 3. Combustion applications of the hard-to-abate sector, related processes and equipments.

Applications	Processes	Equipments
Food	Hot water production, Steam production, Drying	Boiler, Cogeneration, Direct flame oven, Dryer
Chemicals	Steam production, Drying, Cracking, Direct heat at high temperature	Boiler, Cogeneration, Direct flame oven, Dryer
Vehicle Production	Varnishing, Environmental heating, Drying, Hardening, Welding, Pressing	Boiler (also at high pressure), Direct flame oven, Dryer
Metals	Steel lamination and melting, Melting of non-ferrous metals, Thermal treatments	Various type of ovens
Refining	Distillation, Reforming, Isomerization, Cracking, Calcination, Hydro-treatment, Catalyst regeneration, Steam production	Oven, Boiler, Cogeneration
Paper	Hot water production, Steam production, Drying, Refining, Finishing	Boiler, Cogeneration, Direct flame dryer
Glass	Raw material melting, Conditioning, Annealing, Moulding, Pressing	Gas oven for melting, Annealing oven
Ceramic	Cooking of raw materials, Drying, Moulding, Finishing	Gas oven, Dryer with recuperated heat, Boiler for hot water
Cement	Cooking of raw materials	Lime kiln: regenerative (parallel fluxes) or vertical kilns (older)
Non metallic minerals	Drying, Melting, Calcination, Evaporation, Separation	Gas dryer, Oven, Boiler, CHP

Table 3 reports combustion-based applications in the hard-to-abate sector.

Producers sell burners (generally working at atmospheric pressure) able to operate up to 100% H₂ usually in the chemical or refining sectors, where a subproduct of hydrogen is produced. Due to the high flame temperature, combustors' material have to be chosen suitably. In fact, the flame can easily attach close to the nozzles, making the choice of materials a serious concern. High frequency noise can be avoided by means of silencers or damping devices. Some burners operating at 100% H₂ are non-premixed to reduce NO_x (for example, in the MILD or flameless combustion regime); others are DLE/DLN premixed. There exist burners without flashback up to 100% H₂.

Almost all glass is produced in furnaces where a mixture of raw materials is combined and melted into a homogeneous mixture. Like many industrial production processes, glass melting can be classified as a continuous or discontinuous (batch) process. The melting point of most glass is around 1400-1600°C, depending on its composition. Consequently, glass production requires a large amount of thermal energy. Because of this high energy demand, glass furnaces are built to minimise heat loss and often feature some form of waste heat recovery system: regenerative, recuperative, electrical. The most commonly used fuels for glass melting furnaces are natural gas, light and heavy fuel oil and liquefied petroleum gas. Methods are currently being investigated to increase the radiative qualities of hydrogen to make it a more viable alternative to natural gas. Traditionally, pure hydrogen has been considered unsuitable for glass melting. This is because the heat produced by its flame is unable to penetrate the liquid glass bath well, leaving the top layer too hot and the bottom too cold. It has always been thought that a glass furnace requires a 'sooty' flame to function, as soot improves radiant heat transfer. Moreover, existing hydrogen combustion systems have not proved suitable for rapid implementation in existing melting furnaces, as major changes in the composition of the furnace atmosphere are expected [56,61]. The influence of these variations on glass chemistry has not yet been adequately studied.

For the lime industry, in the most advanced dry process, raw materials are calcined at around 900-1250°C in a pre-calciner to transform the limestone into lime, which releases CO₂ as a by-product. The materials are then fed into a rotary kiln, where they aggregate to form clinker at 1450°C with flame temperatures reaching 2000°C. The fuel can be coal gas or hydrogen-rich syngas. In the lime industry, the water content of the flue gas would pose a significant challenge [56]. Calcium oxide in fact reacts with steam, causing problems with the quality, efficiency, durability and safety of the product.

Besides being used as a reducing agent, hydrogen has great potential as a fuel in the steel production process. Possible applications of hydrogen mainly concern the production of pellets,

the sintering process, reheating and heat treatment furnaces. Several manufacturers of combustion systems for the steel industry already market some MILD or Flameless type furnaces, which have been successfully tested with a variety of mixtures of natural gas and hydrogen, up to 100% hydrogen. In the MILD combustion mode, the heat release is distributed over a large volume, ensuring an even heat distribution, which is very effective for the material being processed. Products available on the market include, for example, TENOVA's TSX series [87] of reheating furnaces with NO_x emissions below 80 mg/Nm³ at 5% O₂, with a furnace temperature of 1250°C; in 2022, TENOVA also built the first industrial furnace with TRKSX combustion systems [88] for heat treatment in MILD mode up to 100% hydrogen, with NO_x emissions compatible with future, more stringent regulatory limits. Among other applications, LINDE has also invested in oxy-combustion, which can reduce both energy consumption and emissions [89]; in 2020, it tested a full-scale MILD oxy-combustion reheating furnace in Sweden with up to 100% hydrogen with its REBOX HyOx combustion system [90].

Roller kilns are often applied in the ceramics industry because they achieve temperature variations more effectively by moving the product through zones of different temperatures along the length of the kiln, rather than periodically heating and cooling the kiln. They also improve productivity by allowing continuous production. In particular, industrial kilns for the production of ceramic tiles are predominantly of the roller type, fuelled by gas. They can be very long (up to 300 m) and have up to several hundred burners along their length. Depending on the type of production, they must be able to maintain a temperature of up to 1250°C, while the silicon carbide (SiC) burner tubes containing the flame are preferably maintained at temperatures below 1300°C. Fuels can be natural gas, LPG, diesel, paraffin and other liquid fuels up to temperatures of 1800°C. In the case of hydrogen, the great challenge concerns the moisture content of the combustion gases, since the ultimate goal of ceramic production is to remove moisture [91].

The use of hydrogen in boilers [92] is common in those sectors where hydrogen is a waste product of chemical processes. Consequently, there are a number of known technological measures for its safe and efficient handling. This concerns in particular piping, nozzles, high-temperature resistant components that come into contact with flames, burner fans and the combustion chamber. A 100% hydrogen-fuelled boiler can be up to 10% larger than a natural gas boiler producing the same output. Flue gas recirculation is generally used to lower the average flame temperature and contain NO_x. To prevent ignition of the mixture in the supply line, the system is equipped with upstream flame breakers. In steam boilers [93], when switching from natural gas to hydrogen, the variation in heat absorption between the radiant/convective sections can be mitigated by regulating the feedwater split between the two sections.

Table 4 briefly compares the applications described above and the barriers/problems for using hydrogen in the device considered.

Table 4. Main applications of the hard-to-abate sector and barriers to hydrogen implementation.

Applications	Equipments	Temperature [°C]	Fuels	Hydrogen barriers 5
Glass	Melting ovens	1400-1600	Natural gas, oil, LPG	Low radiative, Unknown effects of the different combustion products emission
Lime	Rotary kilns	1450-2000	Coal gas, H ₂ -rich syngas	Higher H ₂ O content in combustion products
Steel	Ovens for heating and thermal treatments	800-1400	Natural gas, coal gas, syngas, LPG	No barriers, for both raw material and combustion emissions
Ceramic	Roller kilns	1250-1800	Natural gas, LPG, diesel, kerosene	Higher H ₂ O content in combustion products
Hot water, steam, drying	Boilers	1200-1400	Natural gas	Volumes higher than 10% for a certain power

5. Conclusions and Future Directions

Hydrogen introduces a remarkable potential for a substantial reduction in CO₂ emissions. Numerous technologies are currently in existence or in development, poised to facilitate the integration of hydrogen into the future energy landscape. While these technologies hold great promise, the primary hurdles lie in achieving the necessary scale and ensuring the economic viability and genuine environmental friendliness of hydrogen generation, distribution, and utilization.

Nowadays, and presumably at least up to 2030, the major issues will not be on the technology but on the hydrogen availability and cost. The current global production of hydrogen is around 70 Mt per year, 99% of them coming from coal and natural gas. If all current hydrogen production would be produced from water electrolysis, the amount of electrical energy required would be around 3600 TWh per year, more than the annual production of the whole European Union [94]. The availability issues will be much more challenging if the electricity for water electrolysis should come from the excess of variable renewable energy sources (VRES) production: the amount of curtailed wind power generation in Germany on 2016 was 4722 GWh, while the energy requirement to produce hydrogen by electrolysis to run just one General Electric 9HA.02 gas turbine for 8000 hours at nominal power is 19600 GWh [63]. Even not introducing the costs issue, just from this perspective, in the authors' opinion the use of blue hydrogen will be mandatory to build a realistic hydrogen value chain, as a precursor of a wide exploitation of green hydrogen when available in practical quantities for an effective CO₂ emission abatement.

In the power sector, gas turbines will persist as a crucial component within the global energy framework, as they complement renewable energy sources and possess a significant existing installed base. They are asked to operate as a back-up service (seasonal and peak) to sustain variable renewable energy sources and stabilize the electric grid (both in voltage and frequency): their contribution to the electric system flexibility is expected to be important even in a 2040 projection (see Figure 12, with an estimate of annual operating hours less than 3000). In this scenario, post-combustion carbon capture technologies are not applicable both from the technical and economic point of view [95]: the potential annual CO₂ reduction due to 100% hydrogen gas turbines is larger than 450 Mt.

Although the long history of gas turbines and their application in different sectors, some research and developments are required for their reliable and safe operation with increasing hydrogen content, to reach at least 80% by volume for a significant CO₂ reduction. Original equipment manufacturers (OEMs) are dedicating substantial resources to incorporating hydrogen-burning technologies into their new engines and crafting modification packages for existing engines.

In the hard-to-abate sector, the reduction of pollutant emission is even more challenging. Electrification cannot be implemented in most industrial processes and hydrogen combustion cannot also be adopted in a straightforward way. In fact, substituting fuel blends with high H₂ content to natural gas, produce changes in radiative energy emission and in exhaust gases composition that can have important effects on the industrial process and the quality of the products. Hence, some research is still needed and more importantly, communication between industries and research should be enhanced, especially in the glass and ceramic sectors. Application of hydrogen in furnaces for the steel industry is instead at an advanced stage.

Behind the technological effort required, the widespread diffusion and availability of H₂ is the real barrier, mainly linked to its production cost. Once accepted hydrogen as part of the solution to the climate change, transition to the "hydrogen society" can only happen starting to build the whole infrastructure and, in the authors' opinion, by using the cheap "blue hydrogen" in the short term, and the still expensive "green hydrogen" in the long term.

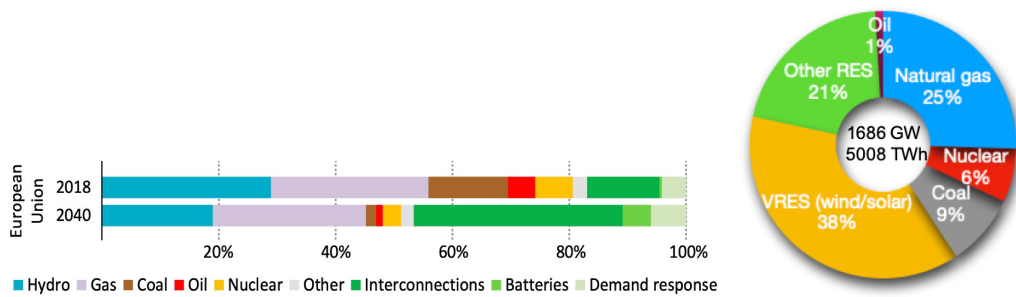


Figure 12. European electric system capacity (Current Policies Scenario) and flexibility sources (Stated Policies Scenario) in the 2040 vision [96].

Author Contributions: Structure, writing, E.G., G.T., A.D., G.M.; sources, all; review, all

Funding: This review study was performed within the Italian project "RICERCA E SVILUPPO DI TECNOLOGIE PER LA FILIERA DELL'IDROGENO POR-H2" ("Research and Development of Technologies for Hydrogen Chain", POR-H2, WP2, LA2.2.5), funded by the Italian Ministry of Environment and Energy Security, under the National Recovery and Resilience Plan (PNRR, Mission 2, Component 2, Investment 3.5, project code I83C22001170006).

Conflicts of Interest: The authors declare no conflict of interest.

References

1. International Energy Agency. Global Hydrogen Review. Technical report, IEA, Paris, 2021.
2. International Energy Agency. Net Zero by 2050 - A Roadmap for the Global Energy Sector. Flagship report, IEA, Paris, 2021.
3. ETN Global. Addressing the Combustion Challenges of Hydrogen Addition to Natural Gas. ETN Position Paper, European Turbine Network, , 2022.
4. Tanaka, Y. and Nakao, M. and Ito, E. and Nose, M. and Saitoh, K. and Tsukagoshi, K.. Development of Low NOx Combustion System with EGR for 780 1700°C-class Gas Turbine. Technical Review 1, MITSUBISHI-HITACHI Heavy Industries, 2013.
5. Ditaranto, M. and Li, H.L. and Lovas, T.. Concept of hydrogen fired gas turbine cycle with exhaust gas recirculation: assessment of combustion 802 and emissions performance. *Int. J. Greenhouse Gas Control* **2015**, 37, 377–383.
6. Ditaranto, M. and Heggset, T. and Berstad, D.. Concept of hydrogen fired gas turbine cycle with exhaust gas recirculation: Assessment of 804 process performance. *Energy* **2020**, 192, .
7. Gersen, S. and Anikin, N.B. and Mokhov, H.B.. Ignition Properties of Methane/Hydrogen Mixtures in a Rapid Compression Machine. *Int. J. Hydrogen Energy* **2008**, 33, 1957–1964.
8. Park, S.. Hydrogen addition effect on NO formation in methane/air lean-premixed flames at elevated pressure. *Int. J. Hydrogen Energy* **2021**, 46, 25712–25725.
9. Sankaran, R. and Im, H.R.. Effects of Hydrogen Addition on the Markstein Length and Flammability Limit of Stretched Methane/Air Premixed Flames. *Combust. Sci. Technol.* **2006**, 178, 1585–1611.
10. Imteyaz, B.A. and Nemitallah, M.A. and Abdelhafez, A.A. and Habib, M.A.. Combustion Behavior and Stability Map of Hydrogen-Enriched Oxy-Methane Premixed Flames in a Model Gas Turbine Combustor. *Int. J. Hydrogen Energy* **2018**, 43, 16652–16666.
11. Nemitallah, M.A. and Imteyaz, B. and Abdelhafez, A. and Habib, M.A.. Experimental and Computational Study on Stability Characteristics of Hydrogen-Enriched Oxy-Methane Premixed Flames. *Applied Energy* **2019**, 250, 433–443.
12. Schefer, R.W.; Wicksall, D.; Agrawal, A.K. Combustion of hydrogen-enriched methane in a lean premixed swirl-stabilized burner. *Proceedings of the combustion institute* **2002**, 29, 843–851.
13. Lieuwen, T.; McDonell, V.; Petersen, E.; Santavicca, D. Fuel flexibility influences on premixed combustor blowout, flashback, autoignition, and stability **2008**.
14. Matalon, M.; Matkowsky, B.J. Flames as gasdynamic discontinuities. *Journal of Fluid Mechanics* **1982**, 124, 239–259.

15. Clavin, P.; Williams, F. Effects of molecular diffusion and of thermal expansion on the structure and dynamics of premixed flames in turbulent flows of large scale and low intensity. *Journal of fluid mechanics* **1982**, *116*, 251–282.
16. ASHINSKY, G.S. Nonlinear analysis of hydrodynamic instability in laminar flames—I. Derivation of basic equations. In *Dynamics of Curved Fronts*; Elsevier, 1988; pp. 459–488.
17. Law, C.K.; Jomaas, G.; Bechtold, J.K. Cellular instabilities of expanding hydrogen/propane spherical flames at elevated pressures: theory and experiment. *Proceedings of the combustion institute* **2005**, *30*, 159–167.
18. Liu, Z.; Yang, S.; Law, C.K.; Saha, A. Cellular instability in $Le < 1$ turbulent expanding flames. *Proceedings of the Combustion Institute* **2019**, *37*, 2611–2618.
19. Creta, F.; Lapenna, P.E.; Lamioni, R.; Fogla, N.; Matalon, M. Propagation of premixed flames in the presence of Darrieus–Landau and thermal diffusive instabilities. *Combustion and Flame* **2020**, *216*, 256–270.
20. Rocco, G.; Battista, F.; Picano, F.; Troiani, G.; Casciola, C.M. Curvature effects in turbulent premixed flames of H₂/air: a DNS study with reduced chemistry. *Flow, Turbulence and Combustion* **2015**, *94*, 359–379.
21. Berger, L.; Attili, A.; Pitsch, H. Synergistic interactions of thermodiffusive instabilities and turbulence in lean hydrogen flames. *Combustion and Flame* **2022**, *244*, 112254.
22. Cecere D. and Giacomazzi E. and Picchia F.R. and Arcidiacono N.M.. Direct Numerical Simulation of a Turbulent Lean Premixed CH₄/H₂-Air Slot Flames. *Combustion and Flame* **2016**, *165*, 384–401.
23. G. Troiani, P. E. Lapenna, F. D'Alessio, and F. Creta. Experimental dataset of H₂/CH₄-air Bunsen flames: interplay of intrinsic instabilities and turbulence. 11th European Combustion Meeting, 2023, pp. 1320–1325.
24. Bechtold, J.; Matalon, M. The dependence of the Markstein length on stoichiometry. *Combustion and flame* **2001**, *127*, 1906–1913.
25. Troiani, G.; Creta, F.; Matalon, M. Experimental investigation of Darrieus–Landau instability effects on turbulent premixed flames. *Proceedings of the Combustion Institute* **2015**, *35*, 1451–1459.
26. Creta, F.; Lamioni, R.; Lapenna, P.E.; Troiani, G. Interplay of Darrieus–Landau instability and weak turbulence in premixed flame propagation. *Physical Review E* **2016**, *94*, 053102.
27. Lapenna, P.E.; Troiani, G.; Lamioni, R.; Creta, F. Mitigation of Darrieus–Landau instability effects on turbulent premixed flames. *Proceedings of the Combustion Institute* **2021**, *38*, 2885–2892.
28. Troiani, G.; Lapenna, P.; Lamioni, R.; Creta, F. Self-wrinkling induced by Darrieus–Landau instability in turbulent premixed Bunsen flames from low to moderately high Reynolds numbers. *Physical Review Fluids* **2022**, *7*, 053202.
29. Lamioni, R.; Lapenna, P.E.; Troiani, G.; Creta, F. Strain rates, flow patterns and flame surface densities in hydrodynamically unstable, weakly turbulent premixed flames. *Proceedings of the Combustion Institute* **2019**, *37*, 1815–1822.
30. Brower, M. and Petersen, E. and Metcalfe, W. and Curran, H.J. and Furi, M. and Bourque, G. and Aluri, N. and Guthe, F.. Ignition Delay Time and Laminar Flame Speed Calculations for Natural Gas/Hydrogen Blends at Elevated Pressures. *ASME Turbo Expo* **2012**, , .
31. Ebi, D. and Jansohn, P.. Boundary Layer Flashback Limits of Hydrogen-Methane-Air Flames in a Generic Swirl Burner at Gas Turbine Relevant Conditions. *Proceedings of ASME Turbo Expo 2020, Turbomachinery Technical Conference and Exposition* **2020**, , . London, England.
32. Beita, J. and Talibi, M. and Sadasivuni, S. and Balachandran, R.. Thermoacoustic Instability Considerations for High Hydrogen Combustion in Lean Premixed Gas Turbine Combustors: A Review. *Hydrogen* **2021**, *2*, 33–57.
33. Xiaoxiao, S. and Abbott, D. and Singh, A.V., Gauthier, P. and Sethi, B.. Numerical Investigation of Potential Cause of Instabilities in a Hydrogen Micromix Injector Array. *Proceedings of ASME Turbo Expo 2021, Turbomachinery Technical Conference and Exposition* **2021**, , .
34. Cecere, D. and G. Carpenella, S. and Giacomazzi, E. and Arcidiacono, N. and Di Nardo, A. and Antonelli, M.. Analisi di Meccanismi Chimici e Fluidodinamici in Fiamme Premiscelate Metano/Idrogeno/Aria. Technical Report D2.2.5.1 of POR-H2 Project, ENEA, 2023.
35. Troiani, G. and Giacomazzi, E. and Marrocco, M. and Di Nardo, A. and Scaccia, S. and Calchetti, G. and Cecere, D. and Assettati, A. and Guidarelli, G. and Stringola, C. and Giulietti, E. and Attanasi, S.. La Combustione di Idrogeno nella Transizione Energetica e Sperimentazione Atmosferica di un Bruciatore con Miscele Metano/Idrogeno in Aria. Technical Report D2.2.5.2 of POR-H2 Project, ENEA, 2023.

36. Altarawneh, M.; Saeed, A.; Al-Harahsheh, M.; Dlugogorski, B.Z. Thermal decomposition of brominated flame retardants (BFRs): Products and mechanisms. *Progress in Energy and Combustion Science* **2019**, *70*, 212–259.

37. Hayakawa, A.; Arakawa, Y.; Mimoto, R.; Somaratne, K.K.A.; Kudo, T.; Kobayashi, H. Experimental investigation of stabilization and emission characteristics of ammonia/air premixed flames in a swirl combustor. *International Journal of Hydrogen Energy* **2017**, *42*, 14010–14018.

38. Cheong, P.; Chang, K.F.; Lai, Y.H.; Ho, S.K.; Sou, I.K.; Tam, K.W. A ZigBee-Based Wireless Sensor Network Node for Ultraviolet Detection of Flame. *IEEE Transactions on Industrial Electronics* **2011**, *58*, 5271–5277. doi:10.1109/TIE.2011.2119455.

39. Djuric, Z.; Radulovic, K.; Trbojevic, N.; Lazic, A. Silicon resonant cavity enhanced UV flame detector. 2002 23rd International Conference on Microelectronics. Proceedings (Cat. No.02TH8595), 2002, Vol. 1, pp. 239–242 vol.1. doi:10.1109/MIEL.2002.1003184.

40. Pauchard, A.; Manic, D.; Flanagan, A.; Besse, P.; Popovic, R. A method for spark rejection in ultraviolet flame detectors. *IEEE Transactions on Industrial Electronics* **2000**, *47*, 168–174. doi:10.1109/41.824139.

41. Starikov, D.; Boney, C.; Pillai, R.; Bensaoula, A. Dual-band UV/IR optical sensors for fire and flame detection and target recognition. ISA/IEEE Sensors for Industry Conference, 2004. Proceedings the, 2004, pp. 36–40. doi:10.1109/SFICON.2004.1287124.

42. Howell, J.; Siegel, R.; Menguc, M. *Thermal Radiation Heat Transfer*, 5th ed.; CRC Press, Taylor & Francis Group, 2010.

43. Modest, M.; Haworth, D. *Radiative Heat Transfer in Turbulent Combustion Systems*; Springer Briefs in Applied Sciences and Technology, Springer, 2016.

44. Caliot, C.; Flamant, G. Pressurized Carbon Dioxide as Heat Transfer Fluid: Influence of Radiation on Turbulent Flow Characteristics in Pipe. *AIMS Energy* **2014**, *3*, 172–182.

45. Zhang, H.; Modest, M. Evaluation of the Planck-Mean Absorption Coefficients from HITRAN and HITEMP Databases. *J. of Quantitative Spectroscopy and Radiative Transfer* **2002**, *73*, 649–653.

46. Rothman, L.e.a. The HITRAN 2008 Molecular Spectroscopic Database. *J. of Quantitative Spectroscopy and Radiative Transfer* **2009**, *110*, 533–572.

47. Rothman, L.; Gordon, I.; Barber, R.; Dothe, H.; Gamache, R.; Goldman, A.; Perevalov, V.; Tashkun, S.; J., T. HITEMP, The High-Temperature Molecular Spectroscopic Database. *J. of Quantitative Spectroscopy and Radiative Transfer* **2010**, *111*, 2139–2150.

48. Wang, L.; Haworth, D.; Turns, S.; Modest, M. Interactions Among Soot, Thermal Radiation, and NO_x Emissions in Oxygen-Enriched Turbulent Nonpremixed Flames: a CFD Modeling Study. *Combustion and Flame* **2005**, *141*, 170–179.

49. Wang, L.; Modest, M.; Haworth, D.; Turns, S. Modeling Nongray Soot and Gas-Phase Radiation in Luminous Turbulent Nonpremixed Jet Flames. *Combustion Theory and Modeling* **2005**, *9*, 479–498.

50. Moss, J.; Stewart, C. Spectrally Resolved Measurements of Radiative Heat Transfer in a Gas Turbine Combustor. *Experimental Thermal and Fluid Science* **2004**, *28*, 575–583.

51. Ebara, T.; Iki, N.; Takahashi, S.; Park, W. Effect of Radiation Reabsorption on Laminar Burning Velocity of Methane Premixed Flame Containing with Steam and Carbon Dioxide. *JSME International Journal Series B - Fluids and Thermal Engineering* **2006**, *49*, 260–264.

52. Mercer, G.; Weber, R. Radiation Enhanced Combustion Wave Speeds. *Proc. R. Soc. London A. The Royal Society*, 1997, Vol. 453, pp. 1543–1549.

53. Cecere, D.; Carpenella, S.; Quaranta, I.; Giacomazzi, E.; Sorrentino, G.; Sabia, P.; Ariemma, G. Large Eddy Simulation of Hydrogen/Air MILD combustion in a cyclonic burner. 10th Turbulence, Heat and Mass Transfer (THMT23); Begell House, I., Ed., 2023. Rome, Italy.

54. Ripoll, J.F.; Pitsch, H. Modelling Turbulence-Radiation Interactions for Large Sooting Turbulent Flames. Annual Research Briefs. Center for Turbulence Research, 2002, pp. 41–52.

55. Turns, S. *An Introduction to Combustion: Concepts and Applications*, 3rd ed.; McGraw-Hill: New York, 2011.

56. Pisciotta, M. and Pilorge, H. and Feldmann, J. and Jacobson, R. and Davids, J. and Swett, S. and Sasso, Z. and Wilcox, J.. Current state of industrial heating and opportunities for decarbonization. *Progress in Energy and Combustion Science* **2022**, *91*, 1–23.

57. Wu, L.; Kobayashi, N.; Li, Z.; Huang, H. Experimental study on the effects of hydrogen addition on the emission and heat transfer characteristics of laminar methane diffusion flames with oxygen-enriched air. *International journal of hydrogen energy* **2016**, *41*, 2023–2036.

58. Michler, T. and Schweizer, F. and Wackermann, K.. Review on the Influence of Temperature upon Hydrogen Effects in Structural Alloys. *Metals* **2021**, *11*, 1–16.

59. Stefan, E. and Talic, B. and Gruber, A. and Peters, T.A.. Materials challenges in hydrogen-fuelled gas turbines. *International Materials Reviews* **2022**, *67*, 461–486.

60. Min'ko, N.I. and Varavin, V.V.. Effect of Water on the Structure and Properties of Glass (Review). *Glass and Ceramics* **2007**, *64*, 3–6.

61. Zier, M. and Stenzel, P. and Kotzur, L. and Stolten, D.. A review of decarbonization options for the glass industry. *Energy Conversion and Management: X* **2021**, *10*, 1–31.

62. International Energy Agency. CO2 Emissions in 2022. Technical report, IEA, 2023.

63. Goldmeer, J. Fuel Flexible Gas Turbines as Enablers for a Low or Reduced Carbon Energy Ecosystem. Technical Report GEA33861, GE Power, 2018.

64. AGORA. Flexibility in thermal power plants. Study , AGORA Energiewende, , 2017.

65. IRENA. Power System Flexibility for the Energy Transition - Part 1: Overview for Policy Makers. Technical Report , International Renewable Energy Agency, , 2018.

66. Gonzalez-Salazar, M.; Kirsten, T.; Prchlik, L. Review of the operational flexibility and emissions of gas- and coal-fired power plants in a future with growing renewables. *Renewable and Sustainable Energy Reviews* **2018**, *82*, 1497–1513.

67. Hidemann, M.; Stevens, M.; Hummel, F. Increased Operational Flexibility from the GT26 (2011) Upgrade. Power-Gen Asia, 2012. Bangkok, Thailand.

68. Zuming, L.; Iftekhar, A. New operating strategy for a combined cycle gas turbine power plant. *Energy Conversion and Management* **2018**, *171*, 1675–1684.

69. Prina, M.; Fanali, L.; Manzolini, G.; Moser, D.; Sparber, W. Incorporating combined cycle gas turbine flexibility constraints and additional costs into the EPLANopt model: The Italian case study. *Energy* **2018**, *160*, 33–43.

70. Larfeldt, J.. *Technology options and plant design issues for fuel-flexible gas turbines*; Vol. Fuel Flexible Energy Generation - Solid, Liquid and Gaseous Fuels, , Woodhead Publishing, 2016. p. 271-291.

71. Kido, H.; Nakahara, M.; Hashimoto, J.; Barat, D. Turbulent Burning Velocities of Two-Component Fuel Mixtures of Methane, Propane and Hydrogen. *JSME International Journal Series B* **2002**, *45*, 355–362.

72. Moccia, V. and D'Alessio, J.. Characterization of CH4-H2-Air mixtures in the high-pressure DHARMA reactor. 25th International Conference on Efficiency, Cost, Optimization (ECOS); , 2012; pp. 287–503.

73. Tuncer, O.; Acharya, S.; Uhm, J. Dynamics and flashback characteristics of confined premixed hydrogen-enriched methane flames. *International J. of Hydrogen Energy* **2009**, *34*, 496–506.

74. AIAA. *Combustion Instabilities in Gas Turbine Engines: Operational Experience, Fundamental Mechanisms, and Modelling*; Vol. 210, AIAA-book, Progress in Astronautics and Aeronautics, 2005.

75. Abbott, D.. Practical examples of the impact of variations in gas composition on gas turbine operation and performance. Gas to Power Europe Forum, 2012.

76. Ferguson, D. and Richard, G.A and Straub, D.. Fuel Interchangeability for Lean Premixed Combustion in Gas Turbine Engines. Proceedings of Turbo Expo: Power for Land, Sea and Air; ASME, , 2009; Number ASME Paper No: GT2008-51261, pp. 973–981.

77. Bruschi R. and Giacomazzi E. and Giulietti E. and Stringola C. and Nobili M. and Pagliaroli T. and Giammartini S.. An Optical Technique for the Identification and Tracking of Combustion Instabilities. 7th Mediterranean Combustion Symposium; The Combustion Institute, , 2011. Chia Laguna, Sardinia, Italy.

78. OXSENSIS. Oxsensis Dynamic Pressure Measurement on a GE 9E Gas Turbine. Technical Review OXC10041, OXSENSIS Ltd., 2020.

79. ETN Global. Proposed NOx Emissions Reporting for Hydrogen-Containing Fuels. ETN Position Paper , European Turbine Network, , 2023.

80. Chiesa, P.; al.. Using Hydrogen as Gas Turbine Fuel. *Journal of Engineering for Gas Turbines and Power* **2005**, *127*, 73–80.

81. ENERGIA, A. Ansaldo Energia solutions for hydrogen combustion: fast-forward to a hydrogen fueled future. Technical report, 2021.

82. Clean Hydrogen Partnership. Clean Hydrogen Joint Undertaking, Strategic Research and Innovation Agenda 2021-2027, Annex to GB decision no. CleanHydrogen-GB-2022-02. Technical report, Hydrogen Europe, 2022.
83. ETN Global. Hydrogen Gas Turbines - The Path Towards a Zero-Carbon Gas Turbine. Technical Report , European Turbine Network, , 2020.
84. Bothien, M.R. and Ciani, A. and Wood, J.P. and Fruechtel, G.. Toward Decarbonized Power Generation With Gas Turbines by Using Sequential Combustion for Burning Hydrogen. *Journal of Engineering for Gas Turbines and Power* **2019**, *141*, 1–10.
85. Funke, H.H.W. and Beckmann, N. and Abanteriba, S.. An overview on dry low NOx micromix combustor development for hydrogen-rich 735 gas turbine applications. *Int. J. of Hydrogen Energy* **2019**, *44*, 6978–6990.
86. Franco, A. and Giovannini, C.. Routes for Hydrogen Introduction in the Industrial Hard-to-Abate Sectors for Promoting Energy Transition. *Energies* **2023**, *16*, 1–23.
87. TENOVA. TSX SmartBurner Burning up to 100 Technical report, 2020.
88. TENOVA. Hydrogen-Ready SmartBurner for Heat Treatment Furnaces. Technical report, 2021.
89. LINDE. REBOX flameless oxyfuel technology. Technical Report 31910_LCS_1017, LINDE AG, Gases Division, , 2017.
90. von Scheele, J.; Zilka, V. Succesful Use of Flameless Oxyfuel in Steel Reheating. METAL 2020, 2020. Brno, Czech Republic.
91. Gomez, R.S.; Gomes, K.C.; Gurgel, J.M.A.M.; Alves, L.B.; Magalhães, H.L.F.; Queiroga, R.A.; Sousa, G.C.P.; Oliveira, A.S.; Vilela, A.F.; Silva, B.T.A.; Vasconcelos, D.B.T.; Brito, G.R.F.; Lima, A.G.B. Investigating the Drying Process of Ceramic Sanitary Ware at Low Temperature. *Energies* **2023**, *16*.
92. ARUP Kiwa. Industrial Boilers - Study to develop cost and stock assumptions for options to enable or require hydrogen- ready industrial boilers. Study 285177-11, ARUP Group Limited, London, 2022.
93. Wang, T.; Zhang, H.; Zhang, Y.; Wang, H.; Lyu, J.; Yue, G. Efficiency and emissions of gas-fired industrial boiler fueled with hydrogen-enriched nature gas: A case study of 108 t/h steam boiler. *International Journal of Hydrogen Energy* **2022**, *47*, 28188–28203.
94. International Energy Agency. The Future of Hydrogen, Sizing today's opportunities. Report prepared by the ieia for the f20, japan, IEA, 2019.
95. AECOM. Start-up and Shut-down times of power CCUS facilities. BEIS research paper, Summary of Study report 2020/031, AECOM, Department for Business, Energy & Industrial Strategy, , 2020.
96. International Energy Agency. World Energy Outlook. Technical report, IEA, 2019.

Disclaimer/Publisher's Note: The statements, opinions and data contained in all publications are solely those of the individual author(s) and contributor(s) and not of MDPI and/or the editor(s). MDPI and/or the editor(s) disclaim responsibility for any injury to people or property resulting from any ideas, methods, instructions or products referred to in the content.